syn-Permethylpentalene Iron and Cobalt Carbonyl Complexes: Proximity Bimetallics Lacking Metal−Metal Bonding

Andrew E. Ashley,[†] Gábor Balázs,[‡] Andrew R. Cowley,[†] Jennifer C. Green,*[,‡] and Dermot O'Hare*[,†]

Chemistry Research Laboratory, University of Oxford, Mansfield Rd, Oxford OX1 3TA, U.K., and Inorganic Chemistry Laboratory, University of Oxford, South Parks Rd, Oxford OX1 3QR, U.K.

Received July 13, 2007

Reaction of 1,3,4,5,6-pentamethyl-2-methylene-1,2-dihydropentalene (Pn*′) with $Fe_2(CO)_9$ or $Co_2(CO)_8$ led to the synthesis of $Fe_2(CO)_5$Pn* (**1**) and $Co_2(CO)_4$Pn* (**2**), respectively, in good yields. **1** and **2** have been structurally characterized by X-ray crystallography and are examples of *syn*-facial 34-electron dinuclear permethylpentalene complexes; **1** contains a μ-CO moiety with an unusual orientation, and NMR data indicate rapid terminal-bridging CO exchange. Theoretical investigations support the structures found in the solid state and also suggest an absence of metal−metal bonding in these compounds, despite the proximity of the metal centers.

Introduction

Transition metal carbonyl compounds have been found to be extremely important in the field of homogeneous catalysis, since dissociative loss of CO can provide active fragments that bind and activate organic molecules toward reaction with desired substrates, e.g., hydroformylation.[1] Pentalene-based metal carbonyls are relatively scarce in the literature,[2] and this can be ascribed to the difficulty in obtaining a hydrocarbon source of the neutral molecule, due to its instability.[3,4] 1,5-Dihydropentalene or the pentalene [2+2] dimer have been reacted with $Fe_2(CO)_9$/$Fe(CO)_5$ either thermally[5] or photochemically,[6] to furnish *syn*-$Fe_2(CO)_5$Pn, albeit in poor yields; this is undoubtedly a result of the thermolability of the hydrocarbon source under the reaction conditions.[7] Stone has used various substituted cyclooctatetraenes to obtain various *syn*-pentalene ruthenium carbonyls based on a triangular $Ru_3(CO)_8$ or $Ru_2(CO)_4(GeMe_3)_2$ core via ring closure of the C_8 carbocycle.[8] $[M(CO_3)]_2(\mu{:}\eta^5{,}\eta^5$-Pn) (M = Mn, Re) have also been formed through metathesis chemistry with the pentalene dianion; the Re compound exists in both *syn* and *anti* forms, whereas for Mn only the *anti*-isomer may be isolated.[9]

Recently we reported the large-scale synthesis of the hydrocarbon 1,3,4,5,6-pentamethyl-2-methylene-1,2-dihydropentalene (Pn*′),[10] which is an isomer of the endocyclic 8π *anti*-aromatic permethylpentalene (Pn*), and its subsequent conversion into the dianion (Li_2Pn*) for use in "anionic" synthon chemistry of Pn*.[11] Herein we wish to report the applicability of Pn*′ as a reagent to introduce the Pn* moiety into organometallic complexes and thus its utility as a neutral synthetic equivalent of this ligand system.

Results and Discussion

The facile reaction of a toluene solution of Pn*′ with excess $Fe_2(CO)_9$ or stoichiometric $Co_2(CO)_8$ at reflux led to the complexes $Fe_2(CO)_5$Pn* (**1**) and $Co_2(CO)_4$Pn* (**2**), respectively, in good (40−60%) yields after a facile workup procedure (Scheme 1). Both materials are moderately air-sensitive crystalline solids that are slightly soluble in aliphatic hydrocarbons yet much more so in aromatic, ethereal, and chlorinated solvents. Single crystals suitable for X-ray crystallography were grown from toluene (**1**) and hexane (**2**) at −78 °C, and views of these complexes are shown in Figures 1and 2.

The Pn* ligand in both compounds is folded away from the metal centers with the "hinge-angle" between their best planes being 6.8° (**1**) and 5.2° (**2**), demonstrating that the steric requirement of the bimetallic unit is not quite accommodated within a planar ring environment and consequent buckling away from the metal centers is observed; the lower value for the Co species parallels the shorter metal−ring centroid distances (Figures 1 and 2), reflecting the smaller size of this metal. The electron count of each metal atom in **1** or **2** could satisfy the 18-electron rule if a metal−metal bond is invoked. Indeed, the Fe1−Fe2 distance is less than that found in the isoelectronic complex *syn*-$Fe_2(CO)_5(\mu{:}\eta^5{,}\eta^5$-COT) [2.742(3) Å; COT = cyclooctatetraene], which is stated to contain a single Fe−Fe bond.[12] However, the corresponding distance in the Co complex is rather long and exceeds the sum of the covalent radius for

* Corresponding authors. E-mail: dermot.ohare@chem.ox.ac.uk; jennifer.green@chem.ox.ac.uk.
[†] Chemistry Research Laboratory.
[‡] Inorganic Chemistry Laboratory.

(1) (a) Crabtree, R. H. *The Organometallic Chemistry of the Transition Metals*; Wiley-Interscience: New York, 2001. (b) Elschenbroich, C.; Salzer, A. *Organometallics: A Concise Introduction, Second, Revised Edition*; VCH: Weinheim, 1992.
(2) Summerscales, O. T.; Cloke, F. G. N. *Coord. Chem. Rev.* **2006**, *250*, 1122.
(3) Hafner, K.; Doenges, R.; Goedecke, E.; Kaiser R. *Angew. Chem., Int. Ed. Engl.* **1973**, *12*, 337.
(4) Bally, T.; Zhu, Z.; Neuenschwander, M.; Chai, S. *J. Am. Chem. Soc.* **1997**, *119*, 1869.
(5) Hunt, D. F.; Russell, J. W. *J. Organomet. Chem.* **1976**, *104*, 373.
(6) Weidemueller, W.; Hafner, K. *Angew. Chem., Int. Ed. Engl.* **1973**, *12*, 925.
(7) Katz, T. J.; Rosenberger, M.; O'Hara, R. K. *J. Am. Chem. Soc.* **1964**, *86*, 249.
(8) Knox, S. A. R.; Stone, F. G. A. *Acc. Chem. Res.* **1974**, *7*, 321.
(9) Jones, S. C.; Hascall, T.; Barlow, S.; O'Hare, D. *J. Am. Chem. Soc.* **2002**, *124*, 11610.
(10) Ashley, A. E.; Cowley, A. R.; O'Hare, D. *Eur. J. Org. Chem.* **2007**, *17*, 2239.
(11) Ashley, A. E.; Cowley, A. R.; O'Hare, D. *Chem. Commun.* **2007**, *15*, 1512.
(12) Fleischer, E. B.; Stone, A. L.; Dewar, R. B. K.; Wright, J. D.; Keller, C. E.; Pettit, R. *J. Am. Chem. Soc.* **1966**, *88*, 3158.

10.1021/om700702v CCC: $37.00
Publication on Web 10/11/2007

Scheme 1. Syntheses of 1 and 2

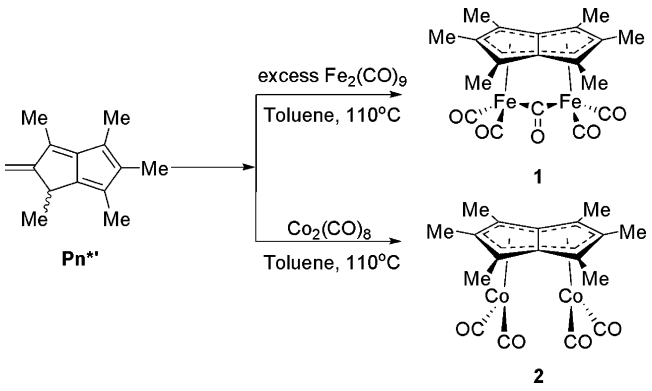

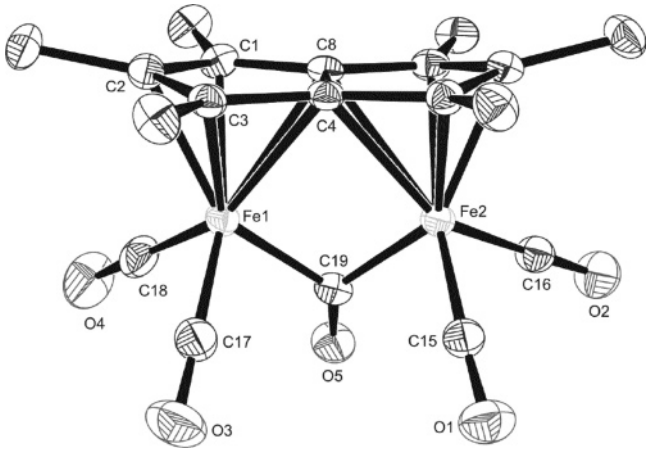

Figure 1. Molecular structure of **1** (hydrogen atoms excluded for clarity, thermal ellipsoids at 50% probability). Selected bond lengths [Å]: Fe1−C1 2.125(3), Fe1−C2 2.087(3), Fe1−C3 2.141(3), Fe1−C4 2.287(3), Fe1−C8 2.289(3), Fe1−C19 1.973(4), Fe2−C19 1.930(3), Fe1−C16 1.755(3), Fe1−C15 1.770(3), Fe2−C17 1.776(3), Fe2−C18 1.743(3), C19−O5 1.182(4), C15−O1 1.148(4), C16−O2 1.153(4), C17−O3 1.151(4), C18−O4 1.157(4), Fe1−Ct 1.814(3), Fe1−Fe2 2.6869(5). Ct is the closest C_5 ring centroid.

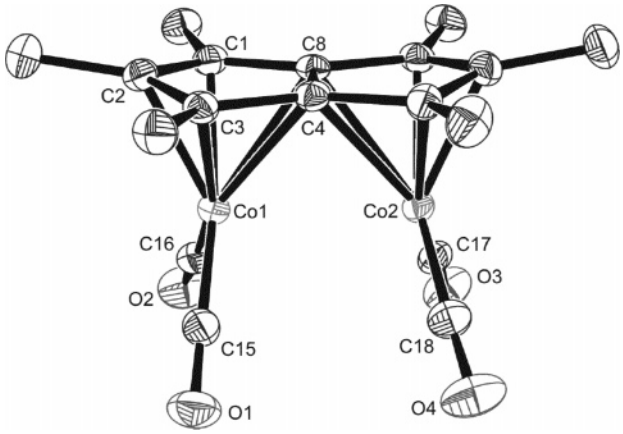

Figure 2. Molecular structure of **2** (hydrogen atoms excluded for clarity, thermal ellipsoids at 50% probability). Selected bond lengths [Å]: Co1−C1 2.070(4), Co1−C2 2.039(4), Co1−C3 2.082(4), Co1−C4 2.287(4), Co1−C8 2.274(4), Co1−C15 1.744(2), Co1−C16 1.752(2), Co2−C17 1.751(2), Co2−C18 1.745(2), C15−O1 1.155(2), C16−O2 1.148(2), C17−O3 1.147(2), C18−O4 1.150(2), Co1−Ct 1.772(4), Co1−Co2 2.675(3). Ct is the closest C_5 ring centroid.

Co (2.32 Å),[13] suggesting almost no metal−metal overlap. A striking difference between **1** and its COT counterpart is the unusual geometry of the bridging CO group, which is perpendicular to the ligand plane in the latter species.

The carbocyclic ring for both compounds does not display the bond alternation pattern characteristic of an *anti*-aromatic species; conversely the intraligand average C−C bond length (1.42−1.44 Å) closely resembles that of benzene (1.40 Å). Thus, it appears that coordination of the metal fragments have resulted in the isomerization and aromatization of the pentalenic framework in Pn*′, analogous to the reaction of 1,2-dichlorocyclobutene with $Fe_2(CO)_9$ to form $Fe(\eta^4\text{-}C_4H_4)(CO)_3$.[14]

The average of the distances M1−C1, M1−C2, and M1−C3 for **1** and **2** is rather shorter than the average for the M−bridgehead carbon atom contacts (C4 and C8), the difference for the former compound being largest (0.24 vs 0.22 Å). This "ring-slip" is analogous to the "indenyl effect" or "ene-allyl" distortion, and this bias toward η^3-bonding shows that a similar effect is operational here.[15] **2** has no analogue in pentalene or COT chemistry. The average Co−C ring distance is slightly longer than in other cyclopentadienyl species, e.g., $Co(C_5H_5)(CO)_2$ (2.07 Å),[16] $Co(C_5Me_5)(CO)_2$ (2.09 Å),[17] and $Co(C_5Ph_5)(CO)_2$ (2.10 Å),[18] but almost identical to the closely related species *syn*-$[Co(CO)_2]_2$-1,3,5,7-tetra-*tert*-butyl-*s*-indacene (2.14 Å).[19] The latter is an example of another bimetallic compound in which the two cobalt dicarbonyl moieties are bound to the same face of the ligand, although the Co atoms are much further apart, separated by a benzenoid ring.

The room-temperature ^{1}H NMR spectrum of **1** and **2** indicates that the Pn* unit is highly symmetrical, displaying two singlets in the expected ratio of 2:1, which implies C_{2v} symmetry for both molecules in solution, and is in agreement with the solid-state data for **2**, but not **1**. Only one ^{13}C carbonyl resonance is detected for both compounds in the room-temperature ^{13}C NMR spectrum; for **1** the chemical shift is intermediate in value between those characteristic of terminal and bridging coordinated CO (at δ = 227 ppm). Variable-temperature ^{1}H NMR down to −100 °C for the latter species did not lead to a change in the chemical shifts, nor was any line broadening observable.

Solid-state IR spectroscopy (KBr) of the Fe bimetallic revealed five stretches for the carbonyl ligands, as anticipated if the molecule is assumed to have C_s symmetry similar to that found by X-ray crystallography. The presence of a band at 1750 cm^{-1} shows the presence of a bridging CO, and it can be concluded that if bridge-terminal carbonyl exchange is indeed occurring in **1**, the frequency of this interconversion must be between 10^8 and 10^{13} Hz, since it cannot be observed on the NMR time scale.

Three carbonyl stretches are seen for the carbonyls in the IR spectrum (CH_2Cl_2) for **2** at 2015, 1973, and 1950 cm^{-1}; the closest structural comparison is with *syn*-$[Co(CO)_2]$-1,3,5,7-tetra-^{t}Bu-*s*-indacene, which exhibits values at 2016, 1994, and 1953 cm^{-1} (THF). From these it can be deduced that the electron-donating power of the Pn* ligand is equivalent to, or even exceeds, that of this alkylated indacene within experimental error.

(13) Emsley, J. *The Elements*; Oxford University Press: Oxford, 1989.
(14) Fitzpatrick, J. D.; Watts, L.; Emerson, G. F.; Pettit, R. *J. Am. Chem. Soc.* **1965**, *87*, 3254−3255.
(15) (a) Calhorda, M. J.; Romao, C. C.; Veiros, L. F. *Chem.−Eur. J.* **2002**, *8*, 868. (b) Smith, M. E.; Andersen, R. A. *J. Am. Chem. Soc.* **1996**, *118*, 11119. (c) O'Connor, J. M.; Casey, C. P. *Chem. Rev.* **1987**, *87*, 307.
(16) Antipin, M. Y.; Struchkov, Y. T.; Chernega, A. N.; Meidine, M. F.; Nixon, J. F. *J. Organomet. Chem.* **1992**, *436*, 79.
(17) Byers, L. R.; Dahl, L. F. *Inorg. Chem.* **1980**, *19*, 277.
(18) Chambers, J. W.; Baskar, A. J.; Bott, S. G.; Atwood, J. L.; Rausch, M. D. *Organometallics* **1986**, *5*, 1635.
(19) Cary, D. R.; Webster, C. G.; Drewitt, M. J.; Barlow, S.; Green, J. C.; O'Hare, D. *Chem. Commun.* **1997**, 953.

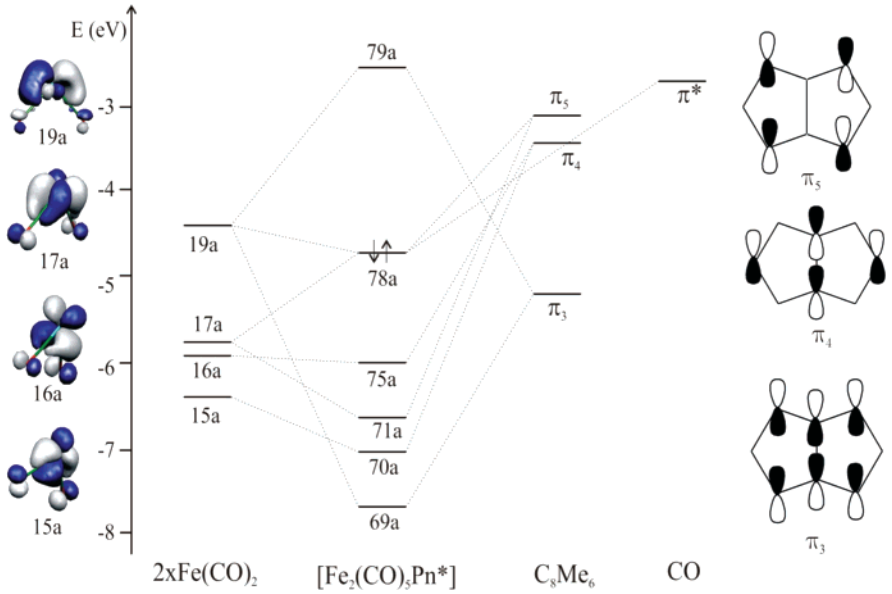

Figure 3. MO diagram for **1** (only energy levels important for Pn* bonding are represented).

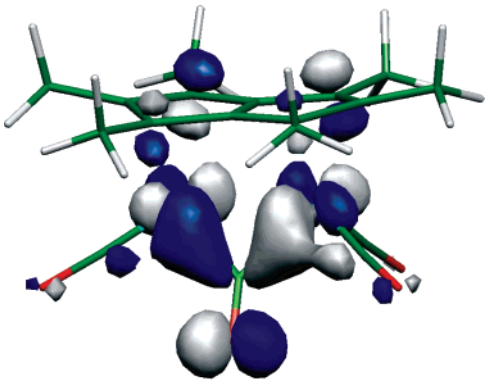

Figure 4. Isosurface of molecular orbital 78a in **1**.

In order to elucidate the electronic structure for both complexes and to ascertain the origin of the unusual side-on geometry of the bridging carbonyl in the Fe species, the molecule was analyzed using DFT calculations. For **1** the geometry optimization was conducted without any geometry restraints and the calculated geometrical parameters are in good agreement with the experimental data; in particular the position of the μ-CO is reproduced very well. Constraint to C_{2v} for **2** gave good optimization parameters in general, although calculated bond lengths were slightly shorter than those experimentally derived, e.g., Co−Co distance of 2.64 Å. The bonding was analyzed by fragment calculations, where the molecules were broken down into two $M(CO)_2$ (M = Fe, Co), a Pn*, and in the case of M = Fe, a CO unit (Figure 3).

The bonding of the Pn* unit to the $Fe(CO)_2$ fragments occurs via the π_3, π_4, and π_5 orbitals of the pentalene fragment. The $Fe(CO)_2$ orbitals implied in the Fe−Pn* bonding contain mainly Fe d-orbital contributions. The π_3 orbital of Pn* mixes only with the 19a orbital of the $Fe(CO)_2$ moieties to give rise to a bonding molecular orbital, 69a. π_4 interacts with 15a and 16a $Fe(CO)_2$ component orbitals to give rise to two bonding molecular orbitals, 70a and 71a, respectively. The antibonding counterpart of 71a, which is occupied, is stabilized by mixing with one of the π^* orbitals of the bridging CO fragment, and also 19a, to give the HOMO 78a. The topology of this molecular orbital can be seen in Figure 4, where it is evident that this interaction is responsible for the orientation of the bridging CO group. For comparison, the unsubstituted complex (which has been synthesized independently by Weidemuller and Hunt yet never structurally authenticated)[5,6] has also been analyzed using the above methods (details included in the Supporting Information); it is isostructural with **1** and has a longer average Fe−C_{ring} bond distance (2.219 vs 2.186 Å), which is consistent with the augmented donor capacity of the Pn ligand as a result of permethylation.

By examining the interaction of the Fe dimer unit with the Pn* and CO ligands, and considering the Fe_2 fragment σ_g, π_u, δ_g orbitals as bonding and σ_u, π_g, δ_u orbitals as antibonding (orbital notation in the $D_{\infty h}$ point group), summation of the electron population in the complex gives a fractional bond order between the metal centers that can be calculated to be −0.29. This negative value suggests that there is a slight repulsion between the Fe atoms, due to the slightly higher population of the antibonding molecular orbitals, and shows that the Fe−Fe distance is controlled by the pentalene ligand, with the overall conclusion that no metal−metal bond is present.

The molecular orbital diagram for **2** is quite similar (Figure 5), but by quantifying the molecular orbital interactions, slight differences between **2** and **1** emerge.

The mixing between the $M(CO)_2$ orbitals and of the pentalene π orbitals is stronger for M = Co than for M = Fe. This has the effect that for example the π_3 character of $14b_2$, the equivalent of MO 69a in **1**, decreases and becomes more bonding when compared to **1**. A similar trend is also observed for $20a_1$ and $14a_2$, the equivalent of 70a and 71a, respectively. With regard to the presence of a metal−metal bond, although the in-phase combination of the orbitals of the two $Co(CO)_2$ fragments gives rise to a strong Co−Co orbital overlap (MO $22a_1$, Figure 6), there is almost no bonding interaction between the Co atoms because the antibonding combination is also occupied (MO $21b_1$, Figure 6).

The low positive value of the atom−atom overlap population (0.045) also suggests a very weak Co−Co interaction. Summation of the fragment occupations gives a fractional bond order that is calculated to be 0.12. This is consistent with the presence of a very weak interaction between Co centers. It should be noted that using the same method as for **2**, a fractional Mo−Mo bond order of 1.86 was calculated for the 34 valence electron species Mo_2Pn_2.[20] To quantify the Co−Co interaction, a topological analysis of the electron density (ρ) by Bader's atoms

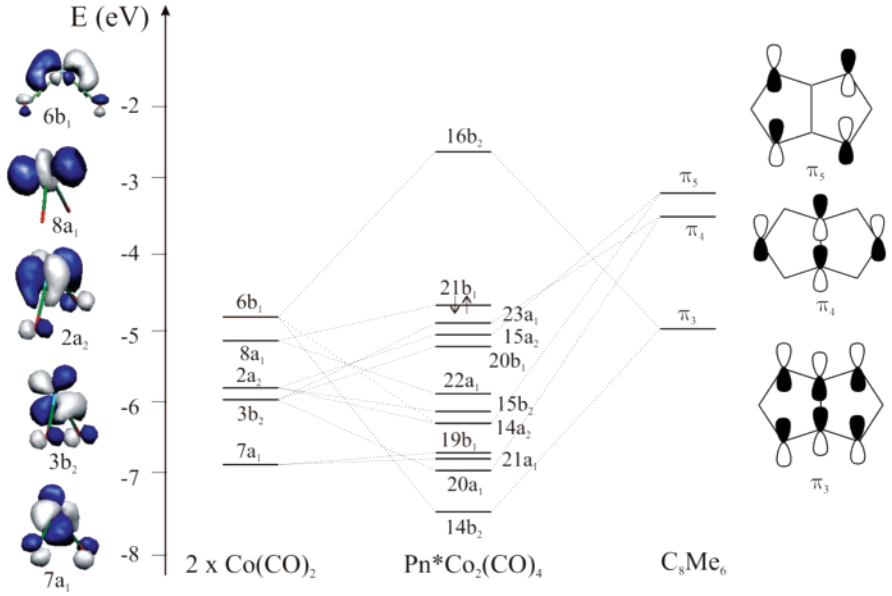

Figure 5. MO diagram for **2**. The orbitals are labeled according to C_{2v} symmetry, for both the $Co(CO)_2$ fragment and **2**.

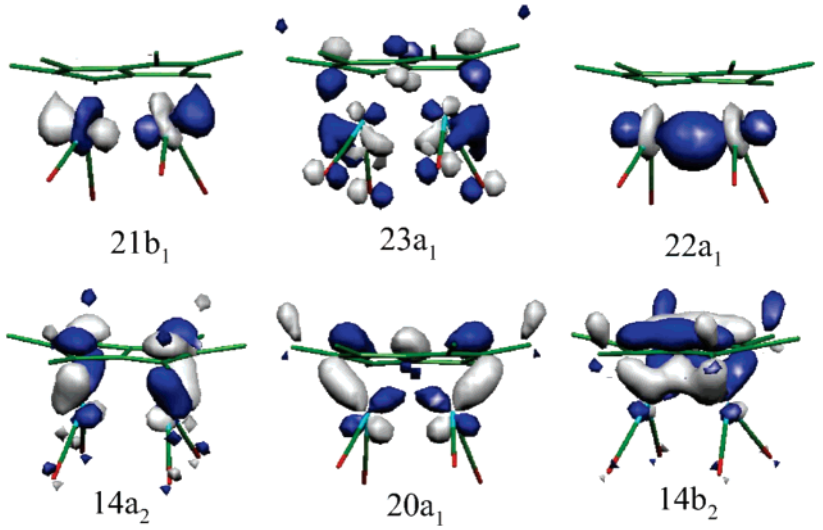

Figure 6. Selected MO isosurfaces for **2** (hydrogen atoms omitted for clarity).

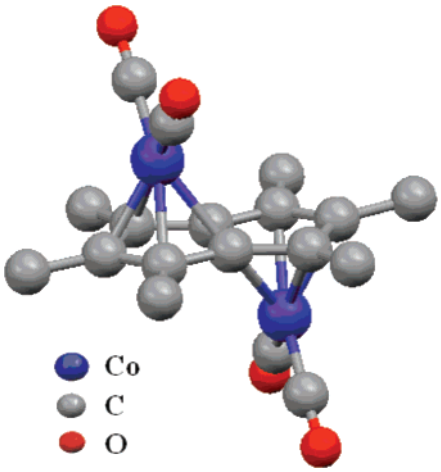

Figure 7. Structure of *trans*-$Co_2(CO)_4Pn^*$, as determined by DFT calculations.

in molecules (AIM) approach[21] was also performed. A bond critical point was found between the two cobalt atoms, but shifted in the opposite direction to the pentalene ring. However, the electronic properties of this point ($\rho(r) = 0.0368$ e/a_o^3, $\nabla^2\rho(r) = 0.0653$ e/a_o^5) suggest a very weak bonding interaction with low $\rho(r)$ and positive $\nabla^2\rho$ values, as characteristic for closed-shell-type interactions. The results of the AIM analysis compare very well with the results of the fragment analysis.

Ab initio computational analysis of the hypothetical isomer *trans*-$Co_2(CO)_4Pn^*$ (Figure 7) shows that the $Co(CO)_2$ moieties now lie closer to an idealized η^5-coordination to each C_5 ring, indicating that the ring-slippage observed in **2** is a result of the repulsion between the *syn*-facial metal centers. Interestingly, the former is found to be 8 kJ mol^{-1} less stable than **2**, this value being within the error of the calculation, and certainly does not confirm the existence of a single bond between the metals (for example, the Co−Co bond enthalpy in $Co_2(CO)_8$ is estimated to be between 64 and 148 kJ mol^{-1}).[22]

Concluding Remarks

In summary, we have demonstrated that the Pn*′ molecule can react with homoleptic carbonyls of Fe and Co to form

(20) Cloke, F. G. N.; Green, J. C.; Jardine, C. N.; Kuchta, M. C. *Organometallics* **1999**, *18*, 1087.
(21) (a) Bader, R. F. W. *Chem. Rev.* **1991**, *91*, 893. (b) Bader, R. F. W. *Atoms in Molecules: A Quantum Theory*; Clarendon Press: Oxford, 1990.
(22) Folga, E.; Ziegler, T. *J. Am. Chem. Soc.* **1993**, *115*, 5169.

permethylpentalene bimetallic carbonyl compounds, where the inorganic fragments are bound to the same face of the ligand; Pn*′ can thus be thought of as a Pn* synthon in reactions of this type. DFT calculations show an overall lack of metal−metal bonding and support the bond distances found in the solid state. These compounds offer a viable opportunity to examine metal−metal cooperativity, especially in catalytic applications. Currently we are extending this new methodology toward the synthesis of other transition metal carbonyl compounds supported by the pentalene nucleus.

Experimental Section

All operations were carried out under a N_2 atmosphere using Schlenk line apparatus and glovebox techniques. Solvents were dried by standard methods and distilled under N_2. The following instrumentation was used: Varian Unity Plus 500 MHz for ^{1}H, ^{13}C NMR spectroscopy; a Perkin-Elmer Paragon 1000 FT-IR spectrometer for infrared measurements. Pn*′ was prepared according to the literature procedure.[18]

Computational Details. Density functional calculations were carried out using the Amsterdam Density Functional program suite ADF 2004.01 or ADF 2005.01.[23] Scalar relativistic corrections were included via the ZORA method for all calculations. The generalized gradient approximation was employed, using the local density approximation of Vosko, Wilk, and Nusair together with the nonlocal exchange correction by Becke and nonlocal correlation corrections by Perdew. TZP basis sets were used with triple-ζ accuracy sets of Slater-type orbitals and two polarization functions added. The cores of the atoms were frozen up to 1s for C and O and 2p for Fe and Co. The AIM (atoms in molecules) analysis was performed with the program Xaim.[24]

X-ray Structure Determination of 1 and 2. Data collection was performed on an Enraf-Nonius FR590 KappaCCD diffractometer. The structures were then solved by direct methods (SIR92) and refined (on F^2) by full-matrix least-squares (CRYSTALS).

Crystal data for **1**: $C_{19}H_{18}O_5Fe_2$, $M_r = 438.04$, crystal size (mm) $= 0.06 \times 0.08 \times 0.30$, monoclinic, $P2_1$, $a = 6.9865(2)$ Å, $b = 14.0121(3)$ Å, $c = 9.2210(2)$ Å, $\beta = 97.5935(8)°$, $V = 894.78(4)$ Å^3, $Z = 2$, $\rho_{calcd} = 1.626$ g cm^{-3}, $\mu = 1.648$ mm^{-1}, Mo Kα radiation ($\lambda = 0.71073$ Å), $T = 150$ K, $2\theta_{max} = 55.0°$, 10 121 measured reflections (3743 independent, $R_{int} = 0.035$), absorption correction (multiscan), transmission factors 0.61/0.91, $R = 0.0283$, $wR = 0.0283$ refined against $|F^2|$, GOF = 1.1224, $[\Delta\rho]_{max}$ 0.71, $[\Delta\rho]_{min}$ −0.59 e Å^{-3}.

Crystal data for **2**: $C_{18}H_{18}O_4Co_2$, $M_r = 416.20$, crystal size (mm) $= 0.12 \times 0.30 \times 0.40$, monoclinic, $P2_1/n$, $a = 9.4915(2)$ Å, $b = 15.5124(2)$ Å, $c = 12.0152(2)$ Å, $\beta = 102.5124(2)°$, $V = 1723.82(5)$ Å^3, $Z = 4$, $\rho_{calcd} = 1.604$ g cm^{-3}, $\mu = 1.942$ mm^{-1}, Mo Kα radiation ($\lambda = 0.71073$ Å), $T = 150$ K, $2\theta_{max} = 55.0°$, 15 397 measured reflections (4069 independent, $R_{int} = 0.026$), absorption correction (multiscan), transmission factors 0.46/0.79, $R = 0.0246$, $wR = 0.0281$ refined against $|F^2|$, GOF = 1.0814, $[\Delta\rho]_{max}$ 0.41, $[\Delta\rho]_{min}$ −0.39 e Å^{-3}.

$Fe_2(CO)_5$Pn* (1). To Pn*′ (1.50 g, 8.05 mmol) in toluene (50 mL) was added $Fe_2(CO)_9$ (4.40 g, 12.1 mmol) against a flush of N_2, and the suspension was heated to reflux, whereupon the solids dissolved and the color changed to red-brown. After 24 h the reaction was cooled, a further portion of $Fe_2(CO)_9$ (5.00 g, 13.7 mmol) added, and reflux resumed. Twenty-four hours later the mixture was cooled and filtered through Celite on a frit, and the solvent was removed under reduced pressure. The dark red residue was then washed with cold (0 °C) pentane (3 × 50 mL) to leave a dark brown solid. This was then recrystallized from toluene/hexane (1:1, 30 mL) at −80 °C to provide **1** as a brown microcrystalline material after two crops (1.59 g, 3.62 mmol, 45%). Anal. (%) Calcd for $C_{19}H_{18}O_5Fe_2$: C 52.10, H 4.14. Found: C 52.17, H 4.22. ^{1}H NMR (C_6D_6): δ 1.35 (s, 12H; Me), 1.43 (s, 6H; Me) ppm. ^{13}C NMR {^{1}H} (C_6D_6): δ 10.0, 10.3 (Me), 65.4, 103.7, 105.7 (quaternary-C), 226.7 (CO) ppm. Selected IR data (KBr): 2006, 1969, 1950, 1922, 1750 (all s, ν(CO)); (CH_2Cl_2): 2014, 1980, 1947, 1750 (all s, ν(CO)) cm^{-1}. MS (EI): *m*/*z* (%) 437.9867 (6) [M$^+$], 410 (18) [M$^+$ − CO], 382 (8) [M$^+$ − 2CO], 354 (27) [M$^+$ − 3CO], 326 (68) [M$^+$ − 4CO], 298 (100) [M$^+$ − 5CO].

$Co_2(CO)_4$Pn* (2). $Co_2(CO)_8$ (2.76 g, 8.05 mmol) was added to Pn*′ (1.50 g, 8.05 mmol) in toluene (50 mL) and heated to reflux. After 24 h the brown solution was cooled and filtered through Celite on a frit, and the solvent was removed under reduced pressure. The dark brown residue was then extracted with chloroform (2 × 30 mL) and filtered, and the solvent was stripped. The resultant solid was then recrystallized from toluene/hexane (1:1, 30 mL) at −80 °C to provide **2** as brown needles. Yield: 62% (2.08 g, 4.99 mmol). Anal. (%) Calcd for $C_{18}H_{18}O_4Co_2$: C 51.94, H 4.39. Found: C 52.04, H 4.37. ^{1}H NMR (C_6D_6): δ 1.36 (s, 12H; Me), 1.82 (s, 6H; Me) ppm. ^{13}C NMR {^{1}H} (C_6D_6): δ 10.5, 11.5 (Me), 68.7, 102.1, 102.2 (quaternary-C), 207.7 (CO) ppm. Selected IR data (KBr): 2014, 1971, 1943 (all s, ν(CO)) cm^{-1} (CH_2Cl_2): 2015, 1973, 1950 (all s, ν(CO)) cm^{-1}. MS (EI): *m*/*z* (%) 415.9877 (5) [M$^+$], 388 (82) [M$^+$ − CO], 360 (90) [M$^+$ − 2CO], 332 (77) [M$^+$ − 3CO], 186 (68) [Pn*$^+$].

Acknowledgment. This study was supported by the UK Engineering and Physical Research Council through a grant award from the EPSRC.

Supporting Information Available: A listing of Cartesian coordinates used in theoretical calculations and CIF files for **1** and **2**. This material is available free of charge via the Internet at http://pubs.acs.org.

OM700702V

(23) *ADF, SCM, Theoretical Chemistry*; Vrije Universiteit: Amsterdam, The Netherlands, http://www.scm.com, and references therein.

(24) Alba, J. C. O.; Jané, C. B. *Xaim;* Departament de Química Física i Inorgànica Universitat Rovira i Virgili Pl. Imperial Tarraco,1 43005, Tarragona, Spain; http://www.quimica.urv.es/XAIM/.